Disulfide Bond Mutagenesis and the Structure and Function of the Head-to-Tail Macrocyclic Trypsin Inhibitor SFTI-1[†,‡]

Michael L. J. Korsinczky, Richard J. Clark, and David J. Craik*

Institute for Molecular Bioscience, University of Queensland, Brisbane, Queensland 4072, Australia

Received August 9, 2004; Revised Manuscript Received November 8, 2004

ABSTRACT: SFTI-1 is a novel 14 amino acid peptide comprised of a circular backbone constrained by three proline residues, a hydrogen-bond network, and a single disulfide bond. It is the smallest and most potent known Bowman−Birk trypsin inhibitor and the only one with a cyclic peptidic backbone. The solution structure of [ABA^{3,11}]SFTI-1, a disulfide-deficient analogue of SFTI-1, has been determined by ^{1}H NMR spectroscopy. The lowest energy structures of native SFTI-1 and [ABA^{3,11}]SFTI-1 are similar and superimpose with a root-mean-square deviation over the backbone and heavy atoms of 0.26 ± 0.09 and 1.10 ± 0.22 Å, respectively. The disulfide bridge in SFTI-1 was found to be a minor determinant for the overall structure, but its removal resulted in a slightly weakened hydrogen-bonding network. To further investigate the role of the disulfide bridge, NMR chemical shifts for the backbone H$^\alpha$ protons of two disulfide-deficient linear analogues of SFTI-1, [ABA^{3,11}]SFTI-1[*6,5*] and [ABA^{3,11}]SFTI-1[*1,14*] were measured. These correspond to analogues of the cleavage product of SFTI-1 and a putative biosynthetic precursor, respectively. In contrast with the cyclic peptide, it was found that the disulfide bridge is essential for maintaining the structure of these open-chain analogues. Overall, the hydrogen-bond network appears to be a crucial determinant of the structure of SFTI-1 analogues.

Sunflower trypsin inhibitor-1 (SFTI-1)[1] is the smallest and most potent known peptidic trypsin inhibitor in the Bowman−Birk (BB) class of proteins (*1*, *2*). The structure of this novel 14 amino acid cyclic peptide has been determined recently both in complex with trypsin (*1*) and free in solution (*3*) and consists of a double-stranded antiparallel β sheet stabilized by a single disulfide bond bridging the β-sheet region. Flanking this sheet at one end is a β-hairpin turn containing two Pro residues, P8 and P9, adopting cis and trans conformations, respectively (binding loop), and at the other end, a second loop containing one Pro residue, P13, in the trans conformation completing the circle (secondary loop) shown in Figure 1. SFTI-1 has an extensive hydrogen-bonding network, as shown in Figure 2, and this, coupled with its cyclic backbone, disulfide bridge, and fixed set of Pro residue conformations, constrains it to adopt a rigid structure (*1*, *3*). SFTI-1 is one of a number of head-to-tail cyclized peptides that have been discovered in recent years from bacteria, plants, and animals (*4*), and there is increasing interest in backbone cyclization for the stabilization of peptides and proteins (*5*).

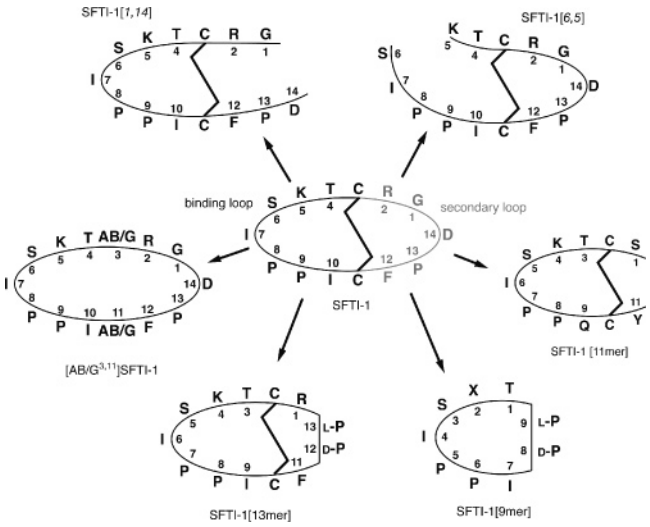

FIGURE 1: Amino acid sequence and schematic structure of SFTI-1 and selected acyclic permutants, disulfide bond variants, and shortened constructs of SFTI-1. Amino acids are shown in one-letter code, and the disulfide bond between residues Cys3 and Cys11 is indicated by a bold line. The binding loop of SFTI-1 is colored black, and the secondary loop is colored gray. Because the peptide backbone is cyclic, the starting point for numbering is arbitrary. Here, Gly1 is chosen based on the initial report by Luckett et al. (*1*). The nomenclature SFTI-1[*n,c*] for acyclic premutants of SFTI-1 denotes (in that order) the position of the N and C termini (*2*). For example SFTI-1[*1,14*] is an acyclic permutant in which the N terminus is Gly1 from the original sequence and the C terminus is Asp14. The peptide [ABA^{3,11}]SFTI-1 has the Cys residues replaced with ABA. SFTI-1[13-mer] and SFTI-1[9-mer] are truncated versions of SFTI-1 having the secondary loop region replaced with a L- and D-Pro. The X denotes Tyr, Phe, or Trp.

† This work was funded by a grant from the Australian Research Council (ARC). D.J.C. is an ARC Professional Fellow.

‡ The atomic coordinates for the solution structure of [ABA^{3,11}]SFTI-1 have been deposited in the Protein Data Bank (accession code 1T9E).

* To whom correspondence should be addressed: Institute for Molecular Bioscience, University of Queensland, Brisbane, Queensland 4072, Australia. Telephone: 61-7-3346 2019. Fax: 61-7-3346 2029. E-mail: d.craik@imb.uq.edu.au.

[1] Abbreviations: ^{1}H NMR, proton nuclear magnetic resonance; 1D, one dimensional; 2D, two dimensional; BAPNA, *N*α-benzoyl-L-arginine *p*-nitroanilide; BB, Bowman−Birk; DQF−COSY, double-quantum-filtered 2D correlation spectroscopy; NOE, nuclear Overhauser effect; NOESY, 2D NOE spectroscopy; MCoTI-II, *Momordica cochinchinensis* trypsin inhibitor-II; RTD-1, *Rhesus theta* defensin-1; SFTI-1, sunflower trypsin inhibitor-1; TOCSY, 2D total correlation spectroscopy; WATERGATE, water suppression by gradient-tailored excitation.

10.1021/bi048297r CCC: $30.25
Published on Web 01/04/2005

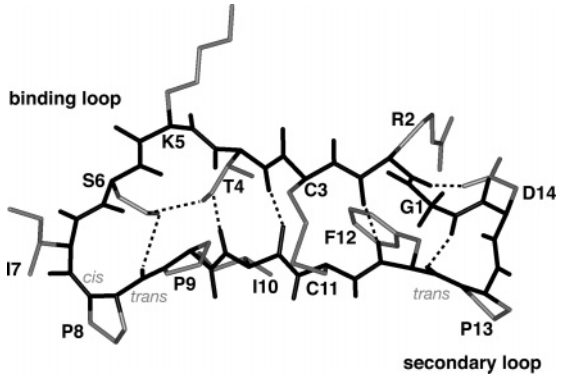

FIGURE 2: Hydrogen bonds in SFTI-1 (pdb code 1JBL). The network of hydrogen bonds stabilizing both loops of the molecule is indicated by dashed lines. The side chains of all residues are colored gray. The Ile7-Pro8, Pro8-Pro9, and Phe12-Pro13 peptide bonds reading from left to right are denoted cis, trans, and trans, respectively.

The high potency and potential applications of SFTI-1 as a molecular scaffold (*2*) have made it the focus of several recent studies. These have been primarily concerned with investigating the importance of its structural elements, namely, the cyclic backbone, hydrogen-bond network, and disulfide bridge. We recently reported (*3*) a comparison of structural and activity features of cyclic SFTI-1 and an acyclic permutant, SFTI-1[*1*,*14*] [nomenclature by Korsinczky et al. (*2*)] shown in Figure 1, that is thought to be topologically related to the putative acyclic precursor of SFTI-1 (*3*) *in vivo*. The secondary loop in SFTI-1[*1*,*14*] is broken between residues G1 and D14. The cyclic and acyclic structures were essentially identical, with the exception of the loss of one hydrogen bond at G1 in the secondary loop of SFTI-1[*1*,*14*], resulting in minimal disordering around the N and C termini. The inhibition potency and hydrolysis rate of SFTI-1[*1*,*14*] were only slightly reduced (*3*, *6*, *7*) relative to SFTI-1, demonstrating that an intact cyclic backbone in the secondary loop is not essential for structural and functional integrity. The disulfide bridge, coupled with the two hydrogen bonds in the secondary loop, provides enough stability to maintain the β sheet in SFTI-1 and in turn the rigidity of the binding loop.

In the absence of the secondary loop though, the potency is significantly reduced. Brauer et al. (*8*) synthesized an 11-residue SFTI-1-like molecule, SFTI-1[11-mer], shown in Figure 1, with a disulfide bond bridging the peptide chain one residue away from the N and C termini. NMR studies (*8*) revealed that the binding loop conformation was almost identical to that in SFTI-1, even with the omission of three residues from the secondary loop. This peptide inhibits trypsin (*9*, *10*) with a potency approximately 50-fold lower than SFTI-1, demonstrating that the absence of the secondary loop lowers the binding affinity even though the binding loop is structurally conserved. It appears that the disulfide bridge, Pro residues, and intramolecular hydrogen-bond network are not as efficient in maintaining the rigidity of the binding loop in the absence of such a secondary brace.

Further evidence that a secondary brace is required to stabilize the disulfide bridge and binding loop was provided by Descours et al. (*11*) who demonstrated that the reduction in potency of the open-chain 11-residue peptide can be restored (*11*) via an alternative linker. They created a new secondary loop by effectively adding a cyclic backbone to SFTI-1[11-mer] using a D- and L-Pro linker, forming a 13-residue bicyclic peptide, SFTI-1[13mer], shown in Figure 1. NMR analysis of this peptide (*11*) revealed that the binding loop was structurally conserved relative to SFTI-1 and the inhibition constant was almost identical to that of SFTI-1. The new secondary brace appears to have maintained the rigidity of the binding loop much like the secondary loop of SFTI-1.

Descours et al. (*11*) explored another variant of SFTI-1 in which they replaced the disulfide bridge and secondary loop with the same D- and L-Pro linker, forming a 9-residue monocyclic peptide, SFTI-1[9-mer], shown in Figure 1. The binding loop structure was essentially conserved, but the peptide displayed a 10-fold reduction in the binding affinity relative to SFTI-1. The reduction in potency most likely resulted from the slightly different conformation in the binding loop where the disulfide was replaced by the Pro linker. This demonstrates for the first time that a secondary brace is potentially not required if the rigidity from the secondary loop, Pro residues, and disulfide bond can be reproduced by using a single bracing loop. The hydrolysis rate of this peptide was not reported.

The stabilizing effect of the secondary loop in SFTI-1 has been studied indirectly in other ways. For example, we recently demonstrated (*12*) that an SFTI-1 acyclic permutant containing an open-chain binding loop, SFTI-1[*6*,*5*] shown in Figure 1, was equally potent to SFTI-1 in *in vitro* trypsin assays. This acyclic permutant has a broken backbone at the position in SFTI-1 corresponding to the scissile bond or trypsin cleavage site in BBI inhibitors. NMR studies demonstrated that the structural conservation in the secondary loop including the disulfide bond allowed hydrogen bonds to form when the open-chain binding loop adopted the native I7−P8 cis orientation, causing SFTI-1[*6*,*5*] to rebind to trypsin. This suggests that the secondary loop may also be a stable independent motif as was found for the binding loop (*13*). It is interesting to hypothesize that it may be sufficiently rigid to maintain the structure of the binding loop and function of SFTI-1 in the absence of the disulfide bridge.

To investigate the role of this disulfide bond in SFTI-1, Jaulent et al. (*6*) and Zablotna et al. (*7*) synthesized the SFTI-1 variants [$G^{3,11}$]SFTI-1 and [$ABA^{3,11}$]SFTI-1, respectively, devoid of a disulfide bridge, shown in Figure 1. Interestingly, replacing the disulfide bridge with two Gly residues causes a 90-fold reduction in potency, whereas replacing it with two amino butyric acid (ABA) residues causes only a 2.4-fold reduction in potency relative to native SFTI-1. The Gly residues may have introduced too much flexibility. In the case of the ABA substitution study, despite the only minor drop in inhibition potency, it was reported that the hydrolysis rate was significantly increased (*7*). The authors mentioned that the binding loop region might be structurally different to SFTI-1 and speculated that the disulfide bridge was more important for the binding affinity than the cyclic backbone. In that study, there was no mention about the hydrogen-bonding network or of what role the disulfide bond may play in other functional analogues of SFTI-1.

In this paper, we have determined the structure of [$ABA^{3,11}$]SFTI-1, a monocyclic variant of SFTI-1. It is found that its solution structure is almost identical to that of SFTI-1

and that the disulfide bond does not play a critical role in maintaining the structure. We also investigated the structures of [ABA^{3,11}]SFTI-1[*6,5*] and [ABA^{3,11}]SFTI-1[*1,14*], disulfide-deficient analogues of the cleavage product and putative precursor of SFTI-1, respectively. It is found that the disulfide bond locks in the orientation of the peptide chain of SFTI-1[*6,5*] and SFTI-1[*1,14*], allowing the formation of hydrogen bonds, and is therefore essential for maintaining the function of its open-chain analogues. The findings for SFTI-1 analogues are compared with other cyclic disulfide-rich peptides from plants and animals and suggest that the sequence of SFTI-1 is particularly well-optimized to have a strong hydrogen-bonding network. The stability of this hydrogen-bond network and the small size of SFTI-1 make it an interesting molecular template for drug design applications.

EXPERIMENTAL PROCEDURES

Solid-Phase Synthesis of [ABA^{3,11}]SFTI-1[6,5], [ABA^{3,11}]-SFTI-1[1,14], and [ABA^{3,11}]SFTI-1. [ABA^{3,11}]SFTI-1[*6,5*] and [ABA^{3,11}]SFTI-1[*1,14*] were assembled using manual solid-phase peptide synthesis with Boc chemistry on a 0.5 mM scale. The C-terminal residue was attached to the resin via a PAM linker (Applied Biosystems, Foster City, CA), and amino acids were added using HBTU with *in situ* neutralization (*14*). The side chains of Asp and Lys were protected with Fm and Fmoc groups, respectively, for [ABA^{3,11}]SFTI-1[*1,14*]. Cleavage of the peptide from the resin was achieved using hydrogen fluoride with *p*-cresol and *p*-thiocresol as scavengers [9:0.5:0.5 (v/v) HF/cresol/thiocresol]. The reaction was allowed to proceed at −5 to 0 °C for 1.5 h; HF was removed under vacuum, and the peptides were precipitated with ether. After cleavage, the peptides were dissolved in 50% acetonitrile containing 0.05% TFA and lyophilised. The crude peptides were purified on a Phenomenex Jupiter 300 C_{18} column. Gradients of 0.05% aqueous TFA and 90% acetonitrile/0.045% TFA were employed with a flow rate of 8 mL/min, and the eluent was monitored at 230 nm. These conditions were used in subsequent purification steps. The Fm and Fmoc protecting groups on the side chains of Asp and Lys in [ABA^{3,11}]SFTI-1[*1,14*] were removed by dissolving the peptide in 1:1 DMF/piperidine and stirring at room temperature for 30 min. The deprotected peptide was purified by RP-HPLC.

[ABA^{3,11}]SFTI-1 was synthesized by dissolving [ABA^{3,11}]-SFTI-1[*1,14*] (22 mg, 0.011 mmol), with the Fm and Fmoc protection of Asp and Lys still present, in DMF (0.1 mg/mL), and a 1−10-fold molar excess of both HBTU and DIEA was added. The reaction mixture was left at room temperature for 5 min and then diluted with 0.05% aqueous TFA and purified using RP-HPLC to yield 12 mg (0.0064 mmol, 58%) of cyclic [ABA^{3,11}]SFTI-1. The Fm and Fmoc side-chain-protecting groups on Asp and Lys, respectively, were removed by dissolving the [ABA^{3,11}]SFTI-1 (12 mg, 0.0064 mmol) in 1:1 DMF/piperdine and stirring at room temperature for 30 min. The reaction mixture was then diluted with 0.05% aqueous TFA and purified by RP-HPLC to yield 8 mg (0.0054 mmol, 84%) of [ABA^{3,11}]SFTI-1.

NMR Spectroscopy. The [ABA^{3,11}]SFTI-1 sample for NMR spectroscopy was dissolved in 90% 20 mM sodium phosphate (H_2O)/10% D_2O at pH 4.5. Spectra were recorded at 290 K on Bruker ARX500 and DMX750 spectrometers with triple-resonance self-shielded z-gradient 5 mm probes. Quadrature detection in the indirect dimension was achieved using TPPI (*15*). A water suppression by gradient-tailored excitation (WATERGATE) (*16*) scheme was used for water suppression. Two-dimensional (2D) total correlation spectroscopy (TOCSY) experiments used the MLEV16 sequence (*17*) for isotropic mixing. The following spectra were recorded on [ABA^{3,11}]SFTI-1: 2D nuclear Overhauser effect (NOE) spectroscopy (NOESY) spectra (*18*) with 4096 × 600 data points in f1 and f2, respectively, and mixing times of 150 and 250 ms; TOCSY spectra (*19*) with 4096 × 512 data points and a spin-lock period of 80 ms; and double-quantum-filtered 2D correlation spectroscopy (DQF−COSY) spectra (*20*) with 4096 × 512 points. Slowly exchanging amide protons were identified by recording a series of one-dimensional (1D) spectra and 2D TOCSY spectra at 290 K over a period of 24 h after dissolution of a fully protonated sample in D_2O.

Structure Calculations for [ABA^{3,11}]SFTI-1. Distance constraints were derived from the intensity of cross signals in NOESY spectra recorded in H_2O or D_2O with a mixing time of 250 ms. Initial structures were generated using X-PLOR 3.851 (*21*). Dihedral angle constraints were derived from stereospecific assignment of side-chain protons according to their NOE patterns. $^3J_{HNH\alpha}$ coupling constants were obtained from line-shape analysis of the antiphase cross-signal splitting in a high digital resolution 2D DQF−COSY spectrum or from a 1D proton nuclear magnetic resonance (^{1}H NMR) spectrum. Distance constraints for hydrogen bonds were generated based on deuterium-exchange data and by examination of structure families calculated without hydrogen-bond constraints. The final 20 structures were calculated using a torsion-angle-simulated annealing protocol within CNS (*22*). The resultant structures were subjected to further molecular dynamics and energy minimization in a water shell (*23*). The final 20 structures with the lowest overall energies were retained for analysis. Structures were visualized using InsightII (Biosym) and MOLMOL (*24*) and analyzed with PROMOTIF (*25*) and PROCHECK-NMR (*26*).

Trypsin Assays. Trypsin assays were carried out according to the method of Erlanger et al. (*27*). Concentrations of [ABA^{3,11}]SFTI-1, [ABA^{3,11}]SFTI-1[*1,14*], and [ABA^{3,11}]-SFTI-1[*6,5*] were determined by amino acid analysis. Trypsin activity was assayed at 25 °C in a 96-well plate with 350 μL of total reaction volume per well, with 42 nM bovine β-trypsin (Type XIII TPCK treated, EC 3.4.21.4) using *N*α-benzoyl-L-arginine *p*-nitroanilide (BAPNA) substrate (1.25 mM) and buffer at pH 8 (50 mM Tris-HCl and 25 mM $CaCl_2$). SFTI-1 inhibitors (0−400 nM) and trypsin were incubated together in buffer for 2 h at 25 °C. The reaction at 25 °C was initiated by addition of the substrate and monitored at 405 nm with readings taken every 60 s for 120 min using a Molecular Devices SpectraMax 250 or a Labsystems Multiskan Ascent. Reactions for each inhibitor concentration were carried out 3 times.

RESULTS

[ABA^{3,11}]SFTI-1, [ABA^{3,11}]SFTI-1[*6,5*], and [ABA^{3,11}]-SFTI-1[*1,14*] were synthesized using solid-phase methods. The three peptides were soluble in water and showed no signs

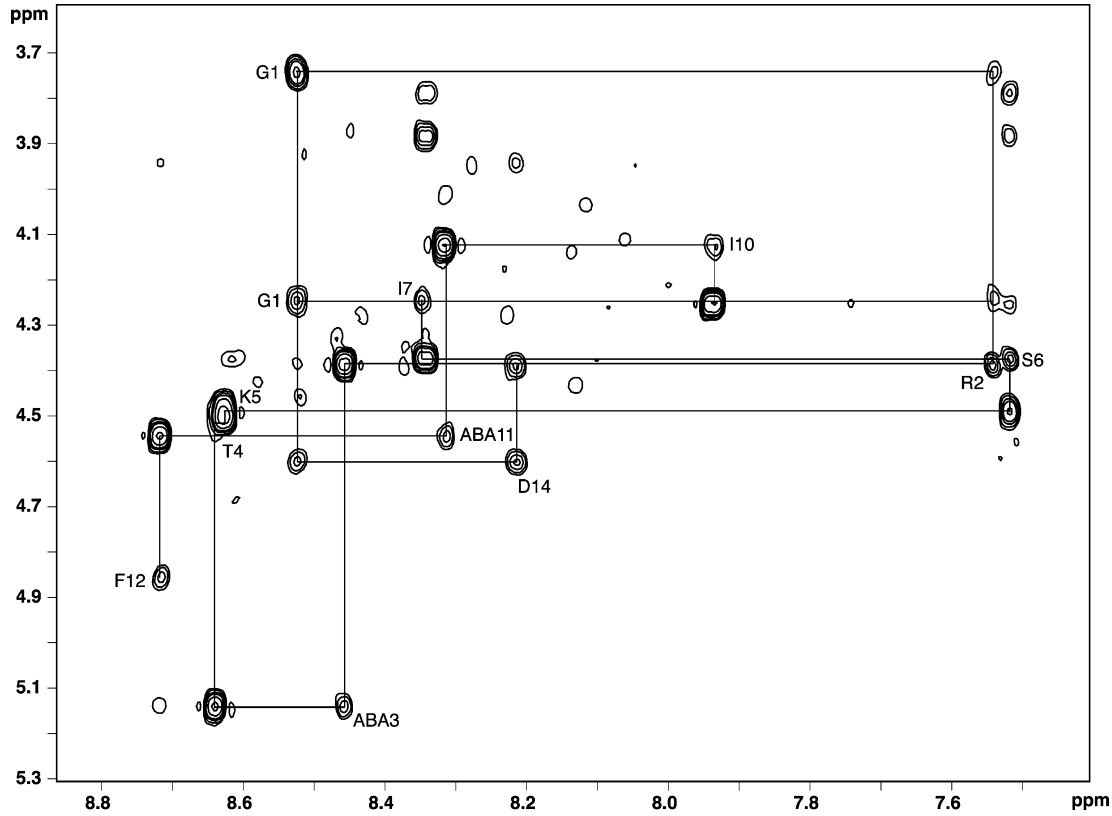

FIGURE 3: Fingerprint region of the NOESY spectrum of [ABA^{3,11}]SFTI-1. The spectrum was recorded at 750 MHz and 290 K (pH 4.5). The sequential connectivity pattern is only broken at the proline residues between I7 and I10 and between F12 and D14.

of aggregation. The NMR spin systems of all individual amino acids were identified and assigned to specific residues using TOCSY, DQF−COSY, and NOESY spectra. By way of example, Figure 3 shows a 750 MHz NOESY spectrum of [ABA^{3,11}]SFTI-1 with the sequential assignments indicated. The cycle of $H^{\alpha}-H^{N}$ sequential connectivities is unbroken apart from the proline residues, demonstrating the cyclic backbone of [ABA^{3,11}]SFTI-1. The NMR data for the Pro residues were used to assign the X-Pro peptide bond conformations. P9 and P13 are in the trans conformation in all of the peptides, as evidenced by strong $H^{\alpha}(i-1)$ Pro-$H^{\delta}(i)$ NOE signals and the absence of $H^{\alpha}(i-1)$ Pro-$H^{\alpha}(i)$ connectivities (*28*). P8 is in the cis conformation in [ABA^{3,11}]-SFTI-1, as evidenced by a strong cross peak between H^{α}-(I7) and H^{α}(P8), but is trans for the other peptides.

Secondary Structure. Secondary chemical shifts (*29*) for the backbone H^{α} protons of [ABA^{3,11}]SFTI-1 in H_2O were calculated as the difference between measured chemical shifts and random-coil values (*30*). Secondary shifts provide a useful first insight into elements of secondary structure present in a peptide. As may be seen from Figure 4, [ABA^{3,11}]-SFTI-1 has many secondary shifts >0.1 ppm, with some approaching 0.8 ppm, indicative of a well-structured peptide. Despite lacking a disulfide bond, the H^{α} shifts of [ABA^{3,11}]-SFTI-1 have a pattern similar to its rigid parent peptide. Much like for SFTI-1, interstrand NOEs between residues R2 and T4 and I10 and F12, as well as large coupling constants ($^3J_{HN-H\alpha} > 8$ Hz) and the consecutive positive H^{α} secondary shifts, indicate the presence of a short antiparallel β sheet. Secondary chemical shifts (*29*) were also calculated for the backbone H^{α} protons of [ABA^{3,11}]SFTI-1[*6,5*] and [ABA^{3,11}]SFTI-1[*1,14*] in H_2O (Figure 4). In contrast with [ABA^{3,11}]SFTI-1, both peptides have random-coil chemical shifts, indicating that they have no defined structure.

A series of hydrogen−deuterium-exchange experiments at 290 K revealed a number of H^{N} protons in [ABA^{3,11}]SFTI-1 that exchange with solvent D_2O over a time scale of several hours. This slow exchange behavior is unusual for such a small peptide and indicates a surprisingly stable hydrogen-bonding network. Slowly exchanging amide protons indicative of strong hydrogen bonds present for >3 h were observed for G1 and R2 and present for >6 h were observed for T4, I10, and F12. The same amide protons in native SFTI-1, whose hydrogen-bond network is stronger still, exchanged approximately 4-fold more slowly. Carbonyl acceptors for each of these protons were unequivocally identified in preliminary structures calculated in the absence of hydrogen-bonding restraints. No slowly exchanging amide protons were detected in [ABA^{3,11}]SFTI-1[*1,14*] or [ABA^{3,11}]SFTI-1[*6,5*], further demonstrating the lack of structure in these peptides. Table 1 summarizes the amide exchange data for the various peptides and also provides comparative data for the parent peptide. The table also summarizes the proline peptide bond conformations deduced from NOE data.

Structure Calculations for [ABA^{3,11}]SFTI-1. A total of 70 distance constraints comprising 31 sequential, 11 medium range and 28 long range NOE contacts, and 5 hydrogen bonds were used for structure calculations. No intraresidual NOEs were included, and the hydrogen-bond restraints were added only after initial structures calculated in the absence of these restraints were used to unequivocally confirm carbonyl acceptor groups matching slowly exchanging amide protons. The stereospecific assignments and χ_1 angles were determined for ABA3 (180°), S6 (60°), ABA11 (180°), F12

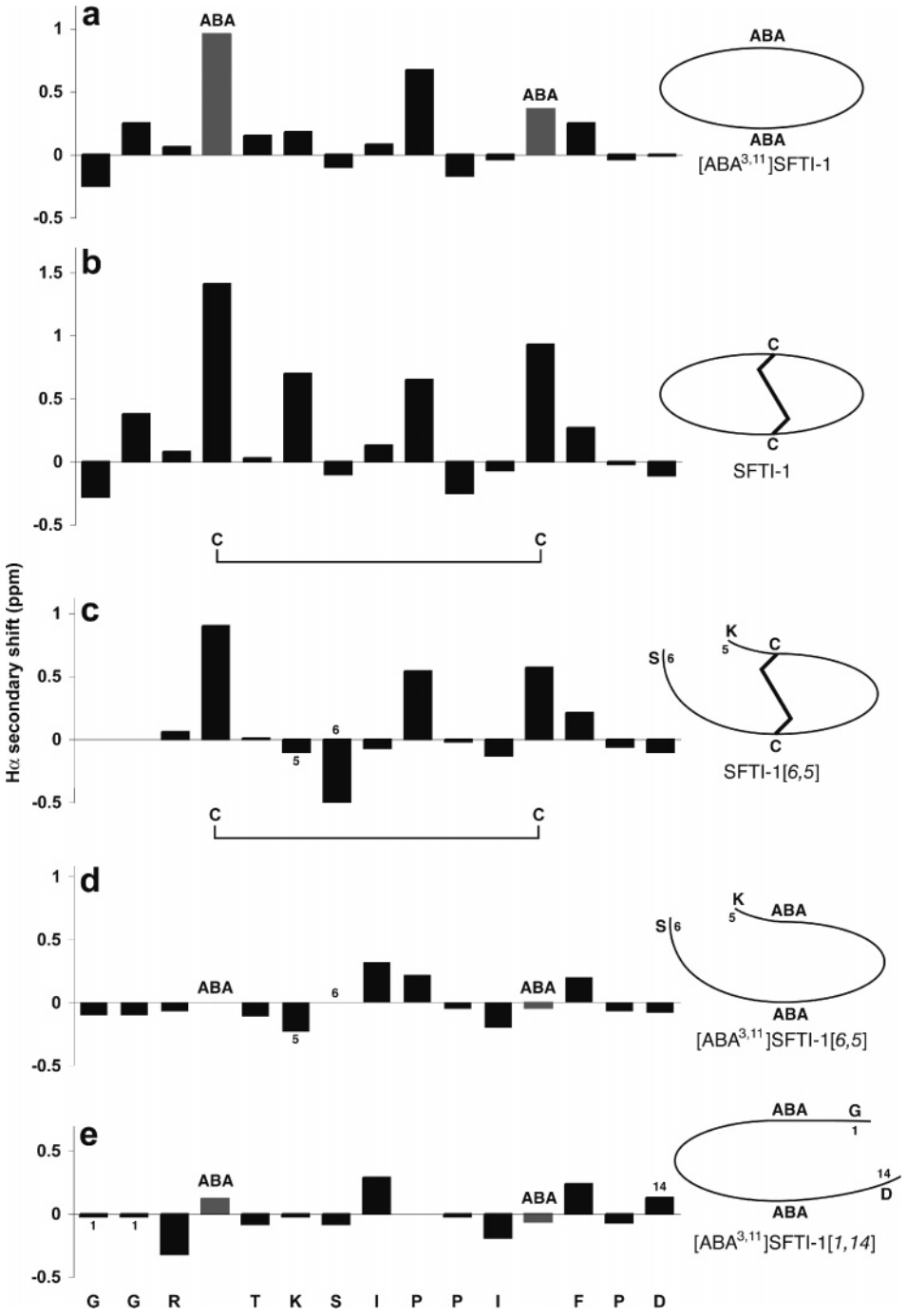

FIGURE 4: H^{α} secondary chemical shifts of [ABA^{3,11}]SFTI-1 and [ABA^{3,11}]SFTI-1[*6,5*] in water (pH 4.5) recorded at 750 MHz and 290 K. Random-coil chemical shifts for ABA were not available; therefore, a pseudo-random-coil value for ABA was calculated using averaged values from [ABA^{3,11}]SFTI-1[*1,14*] and [ABA^{3,11}]SFTI-1[*6,5*]. The assumption is that [ABA^{3,11}]SFTI-1[*1,14*] and [ABA^{3,11}]SFTI-1[*6,5*] are essentially random-coil peptides, making H^{α} shift values of the ABA residues appropriate to use as pseudo-random-coil values.

(−60°), and D14 (60°) based on coupling constants and NOE patterns. Finally, seven ϕ angle constraints of $-120 \pm 40°$ were inferred from $^{3}J_{NH-H\alpha}$ couplings >8 Hz for ABA3, T4, K5, I7, I10, ABA11, and F12. From the 50 structures calculated, 20 were selected based on low overall energy and low constraint violations to represent the solution structure of [ABA^{3,11}]SFTI-1. All structures satisfied the experimental constraints with only minor deviations from the idealized covalent geometry (Table 2).

Figure 5 shows the ensemble of solution structures of [ABA^{3,11}]SFTI-1 superimposed over the backbone atoms of all residues. The mean root-mean-square deviation (rmsd) from the average structure is 0.26 ± 0.09 Å for the backbone atoms and 1.10 ± 0.22 Å for all heavy atoms. An examination of the ϕ and ψ angles shows that [ABA^{3,11}]SFTI-1 adopts the structure of an extended antiparallel β sheet whose strands are joined by an extended loop and one β turn. The presence of a cis peptide bond between residues I7 and P8 causes a bulge in the second β strand. The two β strands adopt a right-handed twist conformation, which is commonly observed for β sheets (*31*).

The solution structure of [ABA^{3,11}]SFTI-1 is similar to that of SFTI-1. Both the overall fold and the dihedral angles of the backbone and side chains of the two structures are nearly

Table 1: Potency, Amide Exchange, and Proline Conformational Data for SFTI-1 and Its Permutants

		sequence												
peptide	potency (nM)[a]	G	R	C	T	K	S	I	P	P	I	C	F	P	D
SFTI-1 (*3*)	0.1−13 (*1*, *3*, *6*−*8*, *11*, *44*)	++[b]	++		+++				cis	trans	+++		+++	trans	
[ABA^{3,11}]SFTI-1	0.24 (*7*)	+	+	A	++				cis	trans	++	A	++	trans	
SFTI-1[*6*,*5*]-isomer 1 (*12*)	0.5 (*12*)	+	+		++				cis	trans	++		++	trans	
SFTI-1[*6*,*5*]-isomer 2 (*12*)	ND								trans	trans				trans	
[ABA^{3,11}]SFTI-1[*6*,*5*]	NA			A					trans	trans	-	A		trans	
SFTI-1[*1*,*14*] (*3*)	0.1−12 (*3*, *6*, *7*)		++		+++				cis	trans	+++		+++	trans	
[ABA^{3,11}]SFTI-1[*1*,*14*]	NA			A					trans	trans		A		trans	

[a] NA and ND denote no trypsin inhibition and no determined trypsin inhibition, respectively. [b] The presence of a slow-exchange amide is represented by + if present after 3 h but less than 6 h, ++ if present after 6 h but less than 24 h, and +++ if present >24 h after dissolution in D_2O.

Table 2: Structural Statistics for the 20 Final Structures of [ABA^{3,11}]SFTI-1

deviations from idealized geometry	
bond lengths (Å)	0.003 ± 0.000
angles (deg)	0.387 ± 0.025
impropers (deg)	0.284 ± 0.027
energies (kcal mol^{-1})	
E_{NOE}	0.73 ± 0.37
E_{dihe}	51 ± 6.8
E_{cdih}	0.01 ± 0.01
E_{vdW}	−25 ± 3.5
$E_{bond} + E_{angle} + E_{improper}$	13 ± 1.7
E_{total}	−501 ± 6.4
restraints violations	
NOE violations > 0.2 Å	0
dihedral violations > 2°	0
rmsd from experimental constraints	
NOE (Å)	0.01 ± 0.004
dihedral angles (deg)	0.11 ± 0.08
pairwise rmsd	
backbone atoms 1−14 (N, Cα, and C) (Å)	0.26 ± 0.09
heavy atoms (Å)	1.10 ± 0.22
Ramachandran statistics (%)	
residues in most favored regions	86
residues in additionally allowed regions	14
residues in disallowed regions	0

identical. The rmsd between the structures is 0.34 ± 0.12 and 1.25 ± 0.26 Å for the backbone and heavy atoms, respectively. Both the binding and secondary loops of [ABA^{3,11}]SFTI-1 are slightly less defined than in SFTI-1, reflecting a smaller number of NOE constraints, probably a result of increased flexibility in the peptide because of the omission of the disulfide bond.

Trypsin Assays. The K_i for inhibition of [ABA^{3,11}]SFTI-1 has previously been reported to be 0.24 nM. Trypsin assays were undertaken for both [ABA^{3,11}]SFTI-1[*1*,*14*] and [ABA^{3,11}]-SFTI-1[*6*,*5*], but both were inactive against trypsin under the same conditions as used for the cyclic peptide.

DISCUSSION

In this study, we have determined the solution structure of [ABA^{3,11}]SFTI-1, a synthetic 14 amino acid cyclic trypsin inhibitor deficient of a disulfide bond relative to the naturally occurring trypsin inhibitor SFTI-1 that is present in sunflower seeds. The structure is surprisingly well-defined and has the same set of proline conformations and a similar hydrogen-bonding network to SFTI-1. Because small peptides lacking disulfide bonds are normally disordered, the remarkable similarity between the two peptides was not expected but helps explain some recent data on the inhibitory activity of the disulfide-deficient peptide.

The distance between the two strands of the β sheet is approximately 0.5 Å wider in [ABA^{3,11}]SFTI-1 than SFTI-1, and the secondary loop is slightly more disordered. This increased disorder most likely reflects increased flexibility caused by the absence of the disulfide bond. The hydrogen-bonding network in [ABA^{3,11}]SFTI-1 is also weakened, as demonstrated by faster amide exchange relative to native SFTI-1. However, the hydrogen bonds and the conformational restraints imposed by the three prolines in [ABA^{3,11}]-SFTI-1 are sufficient to maintain a structure very similar to that of SFTI-1. The similar structure but reduction in rigidity of [ABA^{3,11}]SFTI-1 relative to SFTI-1 would explain the reduction in trypsin inhibition potency (*7*). The structure of SFTI-1 when in complex with trypsin is almost identical to the unbound solution structure (*1*, *3*). While the same functional groups that contribute enthalpically to binding are present in both molecules the more flexible [ABA^{3,11}]SFTI-1 would presumably experience a greater loss of entropy on binding to trypsin than SFTI-1, which could explain its reduced potency. Such entropic losses in binding energy are well-established in ligand macromolecule interactions (*32*). Overall, it appears that the disulfide bond is not crucial for determining the three-dimensional structure and activity of SFTI-1 but serves to reinforce a structure that is defined largely by a network of hydrogen bonds and proline conformations.

The hydrogen-bond network in [ABA^{3,11}]SFTI-1, as demonstrated by the amide-exchange experiments, coupled with its well-defined solution structure determined in this study help explain the similar high potency toward trypsin of a synthetic 71 amino acid BB inhibitor, [A^{14,22}]BBI, also devoid of a trypsin loop disulfide bond (*33*). Removal of the disulfide bond resulted in its trypsin-binding loop essentially expanding from 9 to more than 15 residues. Interestingly, this modification to BBI only resulted in a 5.4-fold reduction in potency, most probably because of the conservation of the I7−P8 and P8−P9 conformations and hydrogen-bond network throughout the loop region, much like in [ABA^{3,11}]SFTI-1.

Because the disulfide bond in SFTI-1 appears not to play a crucial role in defining the structure, what then is its main function? Because inhibition of trypsin by SFTI-1 is an equilibrium reaction, it was important to investigate the role of the disulfide bond in the cleavage product, SFTI-1 [*6*,*5*]. We previously solved the structure of this peptide and showed that the disulfide bond appears to anchor the binding loop of the cleaved peptide, allowing it to adopt the correct conformation to remain active against trypsin. In the current study, we tested this hypothesis by synthesizing [ABA^{3,11}]-

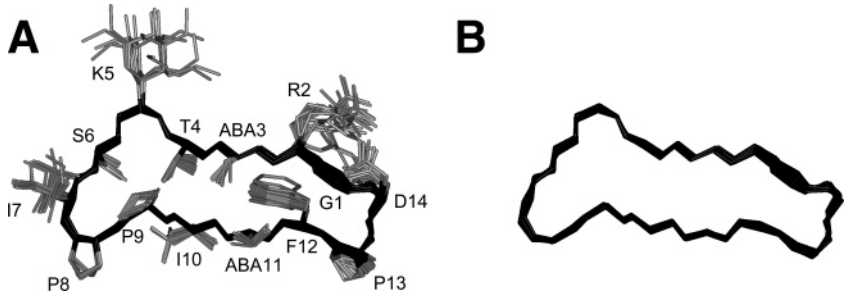

FIGURE 5: Ensemble of 20 structures of [ABA^{3,11}]SFTI-1 superimposed over backbone and heavy atoms of all residues, (A) with and (B) without side-chain residues. The molecules are shown in stick form with the side chains colored gray and the backbone colored black.

SFTI-1[*6,5*], a disulfide-deficient analogue of SFTI-1[*6,5*]. A comparison of H^{α} secondary shifts of SFTI-1[*6,5*] and [ABA^{3,11}]SFTI-1[*6,5*] together with the measurement of their activities demonstrates that the loss of the disulfide bridge causes the peptide to lose its structure as well as its ability to inhibit trypsin. On the basis of the combined results, it appears that the main role of the disulfide bond in SFTI-1 is to minimize hydrolysis by anchoring SFTI-1[*6,5*] such that the hydrogen bonds can maintain structural integrity. The low hydrolysis rate for SFTI-1, higher hydrolysis rate of [ABA^{3,11}]SFTI-1 (*7*), and the lack of trypsin inhibition activity of [ABA^{3,11}]SFTI-1[*6,5*] shown here support this suggestion.

The disulfide bridge in SFTI-1 might also have the additional function of protecting it from other proteases *in vivo*. We have shown that SFTI-1[*1,14*] is a very potent acyclic permutant of SFTI-1, maintaining its activity even with a cleaved secondary loop (*3*). To investigate the role of the disulfide bond in SFTI-1[*1,14*], we synthesized [ABA^{3,11}]SFTI-1[*1,14*], a disulfide-deficient analogue. A comparison of H^{α} secondary shifts of SFTI-1[*1,14*] and [ABA^{3,11}]SFTI-1[*1,14*] revealed a total loss of secondary structure and associated hydrogen-bonding network when the disulfide bond is removed. Inhibition studies also showed that [ABA^{3,11}]SFTI-1[*1,14*] is inactive against trypsin, demonstrating that the disulfide bond is integral to activity in the linear analogue. This may have significant implications for the *in vivo* activity of SFTI-1 in that the disulfide bond may function to prolong the trypsin inhibitory activity of SFTI-1 in the presence of other proteases in its *in vivo* environment. That is, SFTI-1 may retain its activity with an open secondary loop after endoproteinase attack only if it retains an intact disulfide bridge as is the case with SFTI-1[*1,14*] (*3*). Furthermore, if exoproteinases subsequently cleave amino acids from the N and C termini of the open secondary loop, the cleaved peptide may still be able to retain activity, as is demonstrated by the inhibitory activity of SFTI-1[11-mer] (*8*).

A third function of the disulfide bond may be to facilitate the biosynthetic cyclization of SFTI-1. We have proposed that SFTI-1[*1,14*] is a possible biosynthetic precursor peptide of SFTI-1 (*2*, *3*). The residues G1 and D14 from SFTI-1[*1,14*] are in close proximity and are spaced ideally for a spontaneous or enzyme-assisted cyclization event to occur. Because the disulfide-deficient analogue, [ABA^{3,11}]SFTI-1[*1,14*], has no defined structure, it seems likely that the disulfide bond needs to be present to anchor the N and C termini of SFTI-1[*1,14*] in close proximity to allow cyclization to occur. This proposal is based on the fact that SFTI-1[*1,14*] is an extremely potent inhibitor of trypsin and that mature SFTI-1 may have evolved from this peptide. To gain further insight into the evolutionary advantages of cyclization, it is useful to examine other examples of naturally occurring cyclic peptides.

SFTI-1 is one example of a growing number of cystine-rich backbone-cyclized peptides that have been discovered over recent years (*4*), including, the cyclotides (*34*), *Momordica cochinchinensis* trypsin inhibitor-II (MCoTI-II) (*35*) and the θ defensins, exemplified by *Rhesus theta* defensin-1 (RTD-1) (*36*, *37*). The θ defensins are most similar in size to SFTI-1 and comprise 18 amino acids, including 6 Cys residues that are connected to form a "ladder" arrangement of disulfide bonds as illustrated in Figure 6. At first, it might be expected that with its extra amount of cross-bracing RTD-1 would have an even more well-defined structure than SFTI-1, but recent NMR studies (*38*) show that this is not the case. RTD-1 has an elongated β-sheet-type structure with two turns at each end. These turns are well-defined in themselves but appear to be mobile with respect to one another. The striking differences in apparent flexibility between SFTI-1 and RTD-1 suggest that the hydrogen-bonding network in SFTI-1 is more optimized to achieve rigidity than that in RTD-1.

The cyclotides (*39*) are twice the size of SFTI-1, comprising roughly 30 amino acids, and have 3, rather than 1, disulfide bonds, which are arranged in a cyclic cystine knot motif (*34*), as illustrated in Figure 6. There are some interesting parallels between studies of acyclic permutants of the cyclotides and the findings reported here for SFTI-1 analogues. In particular, in the cyclotides, breaking the cyclic backbone does not greatly perturb the overall structure provided that the backbone segments associated with the embedded ring of the cystine knot motif are not broken (*40*). For the cyclotides, it appears that the cystine knot motif is particularly important in defining the compact fold of these molecules, although one disulfide can be removed without greatly perturbing the structures, much like in SFTI-1 (*41*).

MCoTI-II also contains a cyclic cystine knot motif but differs from other cyclotides in its peptide sequence and indeed is more homologous to the knottin family of acyclic squash trypsin inhibitors (*42*). Interestingly, the region in the backbone where the termini of the homologous acyclic inhibitors are putatively joined to form the cyclic peptide is quite disordered in the ensemble of NMR structures (*35*, *43*). Because of this disorder, entropic factors are unlikely to be the primary driving force for the evolution of this family of cyclic peptides (*43*). Rather, protection against attack by exopeptidases has been suggested as the most likely evolu-

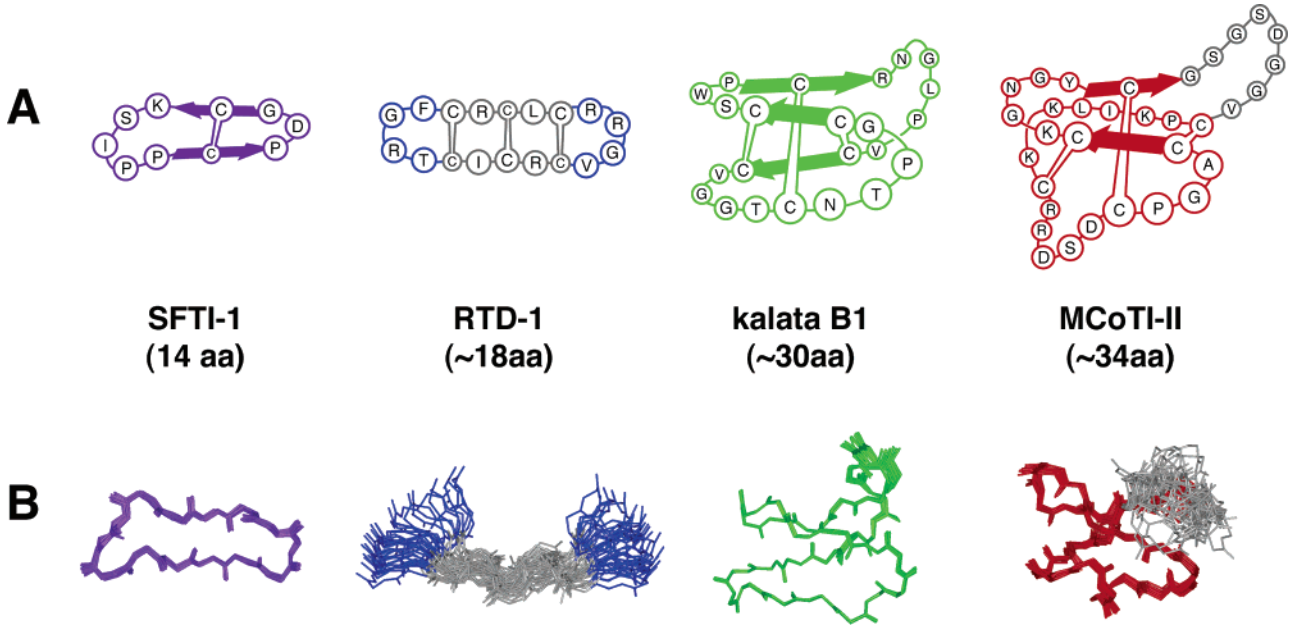

FIGURE 6: Sequence and structural comparison of cyclic peptides related to SFTI-1. A is a schematic of SFTI-1 (purple), RTD-1 (blue), kalata B1 (green), and MCoTI-II (red), respectively. Amino acid residues not involved in secondary structure are shown as letters in circles. Disulfide bonds are represented by lines joined to circles containing Cys residues, and β-sheet structure is represented by filled arrows. B shows the same peptides as the solution structures in stick form colored with respect to the schematic peptides. Flexible regions in the peptides are colored gray. RTD-1 is shown side-on to highlight the relative flexibility of the molecule.

tionary advantage of MCoTI peptides over their acyclic squash family cousins.

It is interesting that SFTI-1 and MCoTI-II, which exemplify two separate classes of trypsin inhibitors (BBI and squash families, repectively), have evolved a strategy for stabilization involving backbone cyclization. Both classes are found in seeds, suggesting that cyclization provides advantages in minimizing proteolytic degradation, given that their putative operational environment in the guts of the predators of the plants is proteolytic. This protective role may also be the case for RTD-1 and the cyclotides.

A comparison of the structural features of the aforementioned four classes of cyclic peptides provides further insight into why SFTI-1 is an extremely rigid molecule and why its disulfide bridge is not required to maintain its structural integrity. While all four molecules contain disulfide bridges and a cyclic backbone, RTD-1 lacks a network of hydrogen bonds and prolines in its sequence, resulting in it having a relatively flexible structure, as shown in Figure 6. This example shows that the presence of a cyclic backbone and multiple disulfide bridges does not guarantee structural rigidity. The combination of the restrictive backbone angles of the proline residues and the hydrogen-bonding network play a significant role in defining the overall structure of SFTI-1.

The results from this study have important repercussions for the design of peptidomimetics or peptidic drugs targeting serine proteases. The rigidity of SFTI-1 is a result of a combination of its cyclic backbone, disulfide bridge, and hydrogen-bonding network. SFTI-1 appears to have a highly optimized design that uses a minimal number of amino acids within the BB class of inhibitors. Its disulfide bridge plays an important role in reducing the hydrolysis of SFTI-1, more so than maintaining its structure. Therefore, designing drugs based solely on the binding loop of SFTI-1 as inhibitors of proteolytic enzymes may not be as simple as previously thought. A tight binding inhibitor would not be effective if it also has a high hydrolysis rate. That is, a short life span of an inhibitor because of rapid degradation would render it useless regardless of its potency. Excising the secondary loop or the disulfide bridge of SFTI-1 reduces its ability to resist hydrolysis. It may well be that SFTI-1 has already been fully optimized for trypsin inhibitory activity and that any further improvement may not be possible. However, redesigning SFTI-1 to target proteolytic enzymes with different mechanisms to the serine proteases may be a promising approach to drug development.

SUPPORTING INFORMATION AVAILABLE

NMR restraints used for the structure determination of [ABA^{3,11}]SFTI-1. This material is available free of charge via the Internet at http://pubs.acs.org.

REFERENCES

1. Luckett, S., Garcia, R. S., Barker, J. J., Konarev, A. V., Shewry, P. R., Clarke, A. R., and Brady, R. L. (1999) High-resolution structure of a potent, cyclic proteinase inhibitor from sunflower seeds, *J. Mol. Biol. 290*, 525−533.
2. Korsinczky, M. L. J., Schirra, H. J., and Craik, D. J. (2004) Sunflower trypsin inhibitor-1, *Curr. Protein Pept. Sci. 5*, 351−364.
3. Korsinczky, M. L., Schirra, H. J., Rosengren, K. J., West, J., Condie, B. A., Otvos, L., Anderson, M. A., and Craik, D. J. (2001) Solution structures by ^{1}H NMR of the novel cyclic trypsin inhibitor SFTI-1 from sunflower seeds and an acyclic permutant, *J. Mol. Biol. 311*, 579−591.
4. Trabi, M., and Craik, D. J. (2002) Circular proteins−No end in sight, *Trends Biochem. Sci. 27*, 132−138.
5. Craik, D. J., Simonsen, S., and Daly, N. L. (2002) The cyclotides: Novel macrocyclic peptides as scaffolds in drug design, *Curr. Opin. Drug Discovery Dev. 5*, 251−260.
6. Jaulent, A. M., McBride, J. D., and Leatherbarrow, R. J. (2001) in *Proceedings of the Second International and Seventeenth American Peptide Symposium* (Lebl, M., and Houghten, R. A., Eds.) pp 547−548, San Diego, CA.

7. Zablotna, E., Kazmierczak, K., Jaskiewicz, A., Stawikowski, M., Kupryszewski, G., and Rolka, K. (2002) Chemical synthesis and kinetic study of the smallest naturally occurring trypsin inhibitor SFTI-1 isolated from sunflower seeds and its analogues, *Biochem. Biophys. Res. Commun. 292*, 855−859.
8. Brauer, A. B., Kelly, G., Matthews, S. J., and Leatherbarrow, R. J. (2002) The ^{1}H NMR solution structure of the antitryptic core peptide of Bowman−Birk inhibitor proteins: A minimal canonical loop, *J. Biomol. Struct. Dyn. 20*, 59−70.
9. Maeder, D. L., Sunde, M., and Botes, D. P. (1992) Design and inhibitory properties of synthetic Bowman−Birk loops, *Int. J. Pept. Protein Res. 40*, 97−102.
10. Domingo, G. J., Leatherbarrow, R. J., Freeman, N., Patel, S., and Weir, M. (1995) Synthesis of a mixture of cyclic peptides based on the Bowman−Birk reactive site loop to screen for serine protease inhibitors, *Int. J. Pept. Protein Res. 46*, 79−87.
11. Descours, A., Moehle, K., Renard, A., and Robinson, J. A. (2002) A new family of β-hairpin mimetics based on a trypsin inhibitor from sunflower seeds, *ChemBioChem 3*, 318−323.
12. Marx, U. C., Korsinczky, M. L., Schirra, H. J., Jones, A., Condie, B., Otvos, L., Jr., and Craik, D. J. (2003) Enzymatic cyclization of a potent Bowman−Birk protease inhibitor, sunflower trypsin inhibitor-1, and solution structure of an acyclic precursor peptide, *J. Biol. Chem. 278*, 21782−21789.
13. Brauer, A. B., Kelly, G., McBride, J. D., Cooke, R. M., Matthews, S. J., and Leatherbarrow, R. J. (2001) The Bowman−Birk inhibitor reactive site loop sequence represents an independent structural β-hairpin motif, *J. Mol. Biol. 306*, 799−807.
14. Schnolzer, M., Alewood, P., Jones, A., Alewood, D., and Kent, S. B. (1992) In situ neutralization in Boc-chemistry solid phase peptide synthesis. Rapid, high yield assembly of difficult sequences, *Int. J. Pept. Protein Res. 40*, 180−193.
15. Marion, D., and Wuthrich, K. (1983) Application of phase sensitive two-dimensional correlated spectroscopy (COSY) for measurements of ^{1}H-^{1}H spin−spin coupling constants in proteins, *Biochem. Biophys. Res. Commun. 113*, 967−974.
16. Sklenar, V., Piotto, M., Leppik, R., and Saudek, V. (1993) Gradient-tailored water suppression for ^{1}H,^{15}N HSQC experiments optimised to retain full sensitivity, *J. Magn. Reson., Ser. A 102*, 241−245.
17. Bax, A., and Davis, D. G. (1985) MLEV-17-based two-dimensional homonuclear magnetization transfer spectroscopy, *J. Magn. Reson. 65*, 355−360.
18. Kumar, A., Ernst, R. R., and Wuthrich, K. (1980) A two-dimensional nuclear Overhauser enhancement (2D NOE) experiment for the elucidation of complete proton−proton cross-relaxation networks in biological macromolecules, *Biochem. Biophys. Res. Commun. 95*, 1−6.
19. Braunschweiler, L., and Ernst, R. R. (1983) Coherence transfer by isotropic mixing: Application to proton correlation spectroscopy, *J. Magn. Reson. 53*, 521−528.
20. Rance, M., Sorensen, O. W., Bodenhausen, G., Wagner, G., Ernst, R. R., and Wuthrich, K. (1983) Improved spectral resolution in COSY ^{1}H NMR spectra of proteins via double quantum filtering, *Biochem. Biophys. Res. Commun. 117*, 479−485.
21. Brunger, A. T. (1992) *X-PLOR Version 3.1 Manual*, Yale University Press, New Haven, CT.
22. Brunger, A. T., Adams, P. D., and Rice, L. M. (1997) New applications of simulated annealing in X-ray crystallography and solution NMR, *Structure 5*, 325−336.
23. Linge, J. P., and Nilges, M. (1999) Influence of non-bonded parameters on the quality of NMR structures: A new force field for NMR structure calculation, *J. Biomol. NMR 13*, 51−59.
24. Koradi, R., Billeter, M. and Wuthrich, K. (1996) MOLMOL: A program for display and analysis of macromolecular structures, *J. Mol. Graphics 14*, 29−32 and 51−55.
25. Hutchinson, E. G., and Thornton, J. M. (1996) PROMOTIF−A program to identify and analyze structural motifs in proteins, *Protein Sci. 5*, 212−220.
26. Laskowski, R. A., Rullmannn, J. A., MacArthur, M. W., Kaptein, R., and Thornton, J. M. (1996) AQUA and PROCHECK-NMR: Programs for checking the quality of protein structures solved by NMR, *J. Biomol. NMR 8*, 477−486.
27. Erlanger, B. F., Kokowsky, N., and Cohen, W. (1961) The preparation and properties of two new chromogenic substrates of trypsin, *Arch. Biochem. Biophys. 95*, 271−278.
28. Wuthrich, K. (1986) *NMR of Proteins and Nucleic Acids*, Wiley-Interscience, New York.
29. Wishart, D. S., and Sykes, B. D. (1994) Chemical shifts as a tool for structure determination, *Methods Enzymol. 239*, 363−392.
30. Wishart, D. S., Bigam, C. G., Holm, A., Hodges, R. S., and Sykes, B. D. (1995) ^{1}H, ^{13}C, and ^{15}N random coil NMR chemical shifts of the common amino acids. I. Investigations of nearest-neighbor effects, *J. Biomol. NMR 5*, 67−81.
31. Chan, A. W., Hutchinson, E. G., Harris, D., and Thornton, J. M. (1993) Identification, classification, and analysis of β-bulges in proteins, *Protein Sci. 2*, 1574−1590.
32. Andrews, P. R., Craik, D. J., and Martin, J. L. (1984) Functional group contributions to drug−receptor interactions, *J. Med. Chem. 27*, 1648−1657.
33. Philipp, S., Kim, Y. M., Durr, I., Wenzl, G., Vogt, M., and Flecker, P. (1998) Mutational analysis of disulfide bonds in the trypsin-reactive subdomain of a Bowman−Birk-type inhibitor of trypsin and chymotrypsin—Cooperative versus autonomous refolding of subdomains, *Eur. J. Biochem. 251*, 854−862.
34. Craik, D. J., Daly, N. L., Bond, T., and Waine, C. (1999) Plant cyclotides: A unique family of cyclic and knotted proteins that defines the cyclic cystine knot structural motif, *J. Mol. Biol. 294*, 1327−1336.
35. Hernandez, J. F., Gagnon, J., Chiche, L., Nguyen, T. M., Andrieu, J. P., Heitz, A., Trinh Hong, T., Pham, T. T., and Le Nguyen, D. (2000) Squash trypsin inhibitors from *Momordica cochinchinensis* exhibit an atypical macrocyclic structure, *Biochemistry 39*, 5722−5730.
36. Tang, Y. Q., Yuan, J., Osapay, G., Osapay, K., Tran, D., Miller, C. J., Ouellette, A. J., and Selsted, M. E. (1999) A cyclic antimicrobial peptide produced in primate leukocytes by the ligation of two truncated α-defensins, *Science 286*, 498−502.
37. Tran, D., Tran, P. A., Tang, Y. Q., Yuan, J., Cole, T., and Selsted, M. E. (2002) Homodimeric θ-defensins from *Rhesus macaque* leukocytes: Isolation, synthesis, antimicrobial activities, and bacterial binding properties of the cyclic peptides, *J. Biol. Chem. 277*, 3079−3084.
38. Trabi, M., Schirra, H. J., and Craik, D. J. (2001) Three-dimensional structure of RTD-1, a cyclic antimicrobial defensin from *Rhesus macaque* leukocytes, *Biochemistry 40*, 4211−4221.
39. Craik, D. J. (2001) Plant cyclotides: Circular, knotted peptide toxins, *Toxicon 39*, 1809−1813.
40. Daly, N. L., and Craik, D. J. (2000) Acyclic permutants of naturally occurring cyclic proteins. Characterization of cystine knot and β-sheet formation in the macrocyclic polypeptide kalata B1, *J. Biol. Chem. 275*, 19068−19075.
41. Daly, N. L., Clark, R. J., and Craik, D. J. (2003) Disulfide folding pathways of cystine knot proteins. Tying the knot within the circular backbone of the cyclotides, *J. Biol. Chem. 278*, 6314−6322.
42. Heitz, A., Chiche, L., Le-Nguyen, D., and Castro, B. (1989) ^{1}H 2D NMR and distance geometry study of the folding of *Ecballium elaterium* trypsin inhibitor, a member of the squash inhibitors family, *Biochemistry 28*, 2392−2398.
43. Felizmenio-Quimio, M. E., Daly, N. L., and Craik, D. J. (2001) Circular proteins in plants: Solution structure of a novel macrocyclic trypsin inhibitor from *Momordica cochinchinensis*, *J. Biol. Chem. 276*, 22875−22882.
44. Long, Y. Q., Lee, S. L., Lin, C. Y., Enyedy, I. J., Wang, S., Li, P., Dickson, R. B., and Roller, P. P. (2001) Synthesis and evaluation of the sunflower derived trypsin inhibitor as a potent inhibitor of the type II transmembrane serine protease, matriptase, *Bioorg. Med. Chem. Lett. 11*, 2515−2519.

BI048297R